An NMR spectrum (C_6D_6) of the orange residue only exhibited resonances for the corresponding *m*- and *p*-tolyl bromide complexes. The ratio of the integrated intensities of the tolyl methyl resonances (meta, δ 2.309, 69%; para, δ 2.279, 31%) was within the experimental limit of error of the ratio of the starting materials (67:33).

Preparation of α,α,α-Trideuterio-2-bromo-*p*-xylene. The compound was prepared in 4 steps from methyl *p*-toluate and used for the preparation of **8a** as previously described.[16] Monobromination of methyl *p*-toluate (3.5 g) with $AlCl_3/Br_2$[34] gave methyl 3-bromotoluate (2.45 g, 46%) as a colorless liquid after Kugelrohr distillation (140 °C (10 mm)). Reduction of the ester (1.29 g) with lithium aluminum deuteride using standard procedures[35] afforded 2-methyl-5-hydroxymethyl-d_2-bromobenzene in 84% yield (0.96 g) after Kugelrohr distillation (110 °C (10 mm)). Treatment of the deuterated alcohol (0.80 g) with PMe_3 in CCl_4[36] followed by solvent removal, ether extraction, and concentration afforded 2-methyl-5-chloromethyl-d_2-bromobenzene in 90% crude yield. Reduction of the crude alkyl chloride with lithium triethylborodeuteride in ether followed by a standard aqueous workup afforded the desired 2-bromo-α,α,α-trideuterio-*p*-xylene in 83% overall yield from the benzylic alcohol. The product was purified by preparative gas chromatography prior to use (6 ft × 1/4 in. 10% SE-30/Chromosorb WAW, 140 °C, 20 mL/min). ^{1}H NMR ($CDCl_3$) δ 2.351 (s, 3 H), 7.001 (dd, J = 7.7, 1.2 Hz, 1 H), 7.105 (d, J = 7.6 Hz, 1 H), 7.358 (d, J = 0.9 Hz, 1 H).

Acknowledgment is made to the donors to the Petroleum Research Fund, administered by the American Chemical Society, to the Camille and Henry Dreyfus Foundation, to the Union Carbide Corporation, to the Chevron Research Company, and to the U.S. Department of Energy (83ER13095) for their support of this work. We also thank Johnson-Matthey, Inc., for a generous loan of rhodium trichloride. We gratefully acknowledge valuable discussions with Prof. R. S. Eisenberg, Prof. J. A. Kampmeier, and Prof. G. McLendon concerning the thermodynamic considerations in this work.

Registry No. 1, 84624-01-1; **2**, 81971-46-2; **2**-d_5, 88704-00-1; **2**-d_5 (ortho isomer), 88704-33-0; **2**-d_5 (meta isomer), 88704-34-1; **2**-d_5 (para isomer), 88704-35-2; **2**-d_6, 84624-02-2; **3**, 88704-01-2; **4**, 84624-03-3; *p*-**6**, 81971-48-4; *m*-**6**, 81971-47-3; **7**, 84624-04-4; **8a**, 88704-02-3; **8b**, 88704-03-4; **10**, 88704-04-5; $(C_5Me_5)Rh(PMe_3)(C{=}\overline{CHCH_2CH_2CH_2})H$, 88704-05-6; $(C_5Me_5)Rh(PMe_3)(\overline{CH{=}CHCH_2CH_2CH_2})$, 88704-06-7; $(C_5Me_5)Rh(PMe_3)[2,5\text{-}C_6H_3(i\text{-}Pr)_2]H$, 88704-07-8; $(C_5Me_5)Rh(PMe_3)(3,5\text{-}C_6H_3Me_2)H$, 88704-08-9; $(C_5Me_5)Rh(PMe_3)(3,4\text{-}C_6H_3Me_2)H$, 88704-09-0; $(C_5Me_5)Rh(PMe_3)(p\text{-}C_6H_4CF_3)H$, 88704-10-3; $(C_5Me_5)Rh(PMe_3)(m\text{-}C_6H_4CF_3)H$, 88704-11-4; $(C_5Me_5)Rh(PMe_3)(m\text{-}C_6H_4OMe)H$, 88704-12-5; $(C_5Me_5)Rh(PMe_3)(p\text{-}C_6H_4OMe)H$, 88704-13-6; $(C_5Me_5)Rh(PMe_3)(o\text{-}C_6H_4OMe)H$, 88704-14-7; $[(C_5Me_5)Rh(PMe_3)(C_6H_5)(THF)]^+[PF_6]^-$, 88704-16-9; $[(C_5Me_5)Rh(PMe_3)(p\text{-tolyl})(THF)]^+[PF_6]^-$, 88704-17-0; $[(C_5Me_5)Rh(PMe_3)(2,5\text{-}C_6H_3Me_2)(THF)]^+[PF_6]^-$, 88704-19-2; $[(C_5Me_5)Rh(PMe_3)(2\text{-}CH_3\text{-}5\text{-}CF_3\text{-}C_6H_3)(THF)]^+[PF_6]^-$, 88704-21-6; $[(C_5Me_5)Rh(PMe_3)(C_6D_5)(THF)]^+[PF_6]^-$, 88704-23-8; $[(C_5Me_5)Rh(PMe_3)(\overline{C{=}CHCH_2CH_2CH_2})(THF)]^-[PF_6]^-$, 88704-25-0; $(C_5Me_5)Rh(PMe_3)Cl_2$, 80298-79-9; $(C_5Me_5)Rh(PMe_3)Br_2$, 88704-26-1; $(C_5Me_5)Rh(PMe_3)I_2$, 88704-27-2; $(C_5Me_5)Rh(PMe_3)(C_6H_5)Cl$, 88704-28-3; $(C_5Me_5)Rh(PMe_3)(C_6H_5)Br$, 81971-44-0; $(C_5Me_5)Rh(PMe_3)(C_6H_5)I$, 88704-29-4; $(C_5Me_5)Rh(PMe_3)(CH_3)Cl$, 84623-98-3; $(C_5Me_5)Rh(PMe_3)(p\text{-tolyl})Br$, 81971-45-1; $(C_5Me_5)Rh(PMe_3)(2\text{-}CH_3\text{-}5\text{-}CD_3\text{-}C_6H_3)Br$, 88704-30-7; $(C_5Me_5)Rh(PMe_3)(C{=}CH)$, 88704-31-8; $Na^+[H_2Al(OCH_2CH_2OCH_3)_2]^-$, 22722-98-1; $Li^+[HBEt_3]^-$, 22560-16-3; $Li^+[HB(sec\text{-}Bu)_3]^-$, 38721-52-7; $K^+[HB(O\text{-}i\text{-}Pr)_3]^-$, 42278-67-1; $AgPF_6$, 26042-63-7; C_6D_5H, 13657-09-5; toluene, 108-88-3; *o*-xylene, 95-47-6; *m*-xylene, 108-38-3; *p*-xylene, 106-42-3; propane, 74-98-6; cyclopentane, 287-92-3; 1,4-di-*tert*-butylbenzene, 1012-72-2; cyclopentene, 142-29-0; α,α,α-trideuterio-2-bromo-*p*-xylene, 88704-32-9; C_6H_6, 71-43-2.

(34) Pearson, D. E.; Stamper, W. E.; Suthers, B. R. *J. Org. Chem.* **1963**, *28*, 3140.
(35) Hooz, J.; Giliani, S. S. H. *Can. J. Chem.* **1968**, *46*, 86.
(36) Gaylord, N. G. "Reduction with Complex Metal Hydrides"; Interscience: New York, 1956.

Stepwise Reductive Acidolysis of $OsH_4(PMe_2Ph)_3$. Mechanism of Hydrogen Elimination/Ligand Addition

Joseph W. Bruno, John C. Huffman, and Kenneth G. Caulton*

Contribution from the Department of Chemistry and Molecular Structure Center, Indiana University, Bloomington, Indiana 47405. *Received September 12, 1983*

Abstract: The polyhydride $OsH_4(PMe_2Ph)_3$ (**1**) reacts with either $HBF_4{\cdot}OEt_2$ or Ph_3CPF_6 and CH_3CN to give $[fac\text{-}Os(PMe_2Ph)_3(CH_3CN)_3]X_2$ (**6**) (X = BF_4, PF_6). The acidolysis reaction proceeds in stepwise fashion through several intermediate species. Using limiting reagent quantities (acid and CH_3CN), it is possible to either isolate or spectrally characterize $OsH_5(PMe_2Ph)_3^+$ (**2**), $OsH_3(PMe_2Ph)_3(CH_3CN)^+$ (**3**), *mer,cis*-$OsH(PMe_2Ph)_3(CH_3CN)_2^+$ (**4**), and *mer*-$Os(PMe_2Ph)_3(CH_3CN)_3^{2+}$ (**5**) on the pathway to **6**. Additionally, kinetic and labeling studies indicate that H_2 substitution by CH_3CN occurs via a preequilibrium H_2 loss and subsequent trapping by CH_3CN. The X-ray diffraction structure of **6** (X = PF_6) is also reported.

The syntheses and certain reaction pathways of transition-metal phosphine polyhydrides are becoming increasingly well developed. This is particularly true for compounds containing third-row transition metals, in addition to various $MoH_4(PR_3)_4$ derivatives.[1] The polyhydrides are characterized by high formal metal oxidation states and coordination numbers, as well as a strong adherence to the 18-electron rule. This latter restriction, coupled with the relative kinetic inertness of third-row compounds, has led to diverse efforts aimed at activating polyhydrides for intermolecular processes. One approach has been complexation with Lewis acids in the hope of enhancing the susceptibility of the transition-metal center to nucleophilic attack;[2-6] it is not always clear that the

(1) Aresta, M.; Sacco, A. *Gazz. Chim. Ital.* **1972**, *102*, 755–870.
(2) (a) Brunner, H.; Wailes, P. C.; Kaesz, H. D. *J. Inorg. Nucl. Chem.* **1965**, *1*, 125–129. (b) Deubzer, B.; Kaesz, H. D. *J. Am. Chem. Soc.* **1968**, *90*, 3276–3277.
(3) Storr, A.; Thomas, B. S. *Can. J. Chem.* **1971**, *49*, 2504–2507.
(4) (a) Shriver, D. F.; Johnson, M. P. *J. Am. Chem. Soc.* **1966**, *88*, 301–304. (b) Shriver, D. F. *Acc. Chem. Res.* **1970**, *3*, 231–238. (c) Richmond, T. G.; Basolo, F.; Shriver, D. F. *Organometallics* **1982**, *1*, 1624–1628.

0002-7863/84/1506-1663$01.50/0

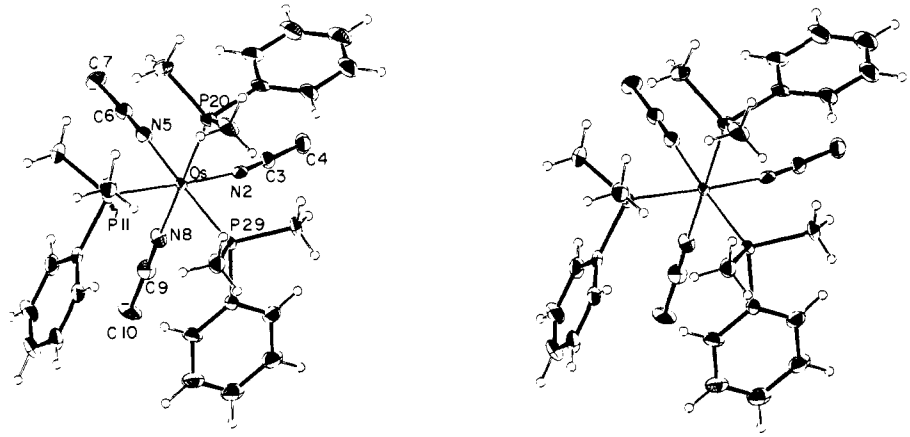

Figure 1. ORTEP stereodrawing of *fac*-$Os(NCMe)_3(PMe_2Ph)_3^{2+}$, showing atom labeling for the inner coordination sphere. This view is down the idealized C_3 axis of the *fac*-OsN_3P_3 unit.

resulting complex is more reactive than its precursor.[5]

More success has been realized in systems designed to create coordinatively unsaturated intermediate fragments. This process is thermally induced in the high-valent $ReH_7(PR_3)_2$, which readily loses H_2 to give (initially) reactive $[ReH_5(PR_3)_2]$.[7,8] For thermally stable polyhydrides, photochemical activation often leads to efficient loss of either H_2[9,10] or coordinated phosphine.[11,12] The usefulness of these approaches has been amply demonstrated in C–H activation processes[7b,c,11b,13-16] and the transformations of unsaturated organics.[7a,d,8]

Two other, somewhat related, means of activating polyhydrides are oxidation[17,18] and acidolysis.[18b,19-22] Although added acid (particularly acids with noncoordinating anions) can lead to simple protonation (eq 1),[20a,22,23] in most cases either oxidation or acidolysis results in multiple loss of hydrides (presumably as H_2) if suitable incoming ligands are available.[16,20,21] As such, reactions of this type are mechanistically complex and seldom lend themselves to elucidation of discrete reaction steps. Herein we report our study of the acidolysis of $OsH_4(PMe_2Ph)_3$,[19a] a system that contradicts the above generalizations only in the sense that it is amenable to detailed mechanistic inquiry. Specifically, we have observed and characterized (to varying extents) several of the intermediate species on the pathway to multiple hydride loss.

Table I. Crystal Data for $[Os(NCMe)_3(PMe_2Ph)_3](PF_6)_2 \cdot CH_2Cl_2$

empirical formula	$OsCl_2P_5F_{12}N_3C_{31}H_{35}$
color	colorless
crystal dimensions, mm	0.12 × 0.12 × 0.13
space group	$P\bar{1}$
cell dimensions (at −160 °C; 42 reflections)	
a, Å	19.653 (4)
b, Å	11.407 (1)
c, Å	10.201 (1)
α, deg	67.03 (1)
β, deg	95.69 (1)
γ, deg	94.96 (1)
molecules/cell	2
volume, Å^3	2092.28
calcd density, g/cm^3	1.736
wavelength, Å	0.71069
mol wt	1093.59
linear absorption coeff, cm^{-1}	34.5
total no. of reflections collected ($6° \leq 2\theta \leq 45°$)	5951
no. of unique intensities	5477
no. of $F > 0.0$	5302
no. with $F > \sigma(F)$	5185
no. with $F > 2.33\sigma(F)$	5023
final residuals	
$R(F)$	0.0506
$R_w(F)$	0.0514
goodness of fit for the last cycle	1.489
maximum Δ/σ for last cycle	0.05

$$MH_xL_y + H^+ \rightarrow MH_{x+1}L_y^+ \quad (1)$$

Results and Discussion

Addition of excess $HBF_4 \cdot OEt_2$ to a CH_2Cl_2/CH_3CN solution of $OsH_4(PMe_2Ph)_3$ (only sparingly soluble in neat CH_3CN) results

(5) Tebbe, F. N. *J. Am. Chem. Soc.* **1973**, *95*, 5412–5414.
(6) (a) Crotty, D. E.; Anderson, T. J.; Glick, M. D.; Oliver, J. P. *Inorg. Chem.* **1977**, *16*, 2346–2350. (b) Aripovskii, A. V.; Bulychev, B. M. *Russ. J. Inorg. Chem. (Engl. Transl.)* **1980**, *25*, 937–938. (c) Aripovskii, A. V.; Bulychev, B. M.; Krivdin, L. B.; Polyakova, V. B. *Ibid.* **1981**, *26*, 1137–1138. (d) Aripovskii, A. V.; Bulychev, B. M.; Polyakova, V. B. *Ibid.* **1981**, *26*, 1458–1461. (e) Protsky, A. N.; Bulychev, B. M.; Solveichik, G. L. *Inorg. Chim. Acta* **1983**, *71*, 35–39.
(7) (a) Baudry, D.; Ephritikhine, M. *J. Chem. Soc., Chem. Commun.* **1980**, 249–250. (b) Baudry, D.; Ephritikhine, M.; Felkin, H. *Ibid.* **1980**, 1243–1244. (c) Baudry, D.; Ephritikhine, M.; Felkin, H. *Ibid.* **1982**, 606–607. (d) Baudry, D.; Ephritikhine, M.; Felkin, H. *J. Organomet. Chem.* **1982**, *224*, 363–376.
(8) Allison, J. D.; Wood, T. E.; Wild, R. E.; Walton, R. A. *Inorg. Chem.* **1982**, *21*, 3540–3546.
(9) (a) Geoffroy, G. L.; Wrighton, M. S. "Organometallic Photochemistry"; Academic Press: New York, 1979. (b) Geoffroy, G. L. *Adv. Chem. Ser.* **1975**, *No. 167*, 181–200.
(10) Green, M. A.; Huffman, J. C.; Caulton, K. G. *J. Organomet. Chem.* **1983**, *283*, C78–C82.
(11) (a) Green, M. A.; Huffman, J. C.; Caulton, K. G. *J. Am. Chem. Soc.* **1981**, *103*, 695–696. (b) Green, M. A.; Huffman, J. C.; Caulton, K. G.; Rybak, W. K.; Ziolkowski, J. J. *J. Organomet. Chem.* **1981**, *218*, C39–C43.
(12) Roberts, D. A.; Geoffroy, G. L. *J. Organomet. Chem.* **1981**, *214*, 221–231.
(13) (a) Janowicz, A. H.; Bergman, R. G. *J. Am. Chem. Soc.* **1982**, *104*, 352–354. (b) Janowicz, A. H.; Bergman, R. G. *Ibid.* **1983**, *105*, 3929–3939.
(14) (a) Crabtree, R. H. *Acc. Chem. Res.* **1979**, *12*, 331–338. (b) Crabtree, R. H.; Mellea, M. F.; Mihelcic, J. M.; Quirk, J. M. *J. Am. Chem. Soc.* **1982**, *104*, 107–113. (c) Crabtree, R. H.; Demou, P. C.; Eden, D.; Mihelcic, J. M.; Parnell, C. A.; Quirk, J. M.; Morris, G. E. *Ibid.* **1982**, *104*, 6994–7001.
(15) (a) Jones, W. D.; Feher, F. J. *J. Am. Chem. Soc.* **1982**, *104*, 4240–4242. (b) Jones, W. D.; Feher, F. J. *Organometallics* **1983**, *2*, 562–563. (c) Fisher, B. J.; Eisenberg, R. *Ibid.* **1983**, *2*, 764–767.
(16) Chatt, J.; Coffey, R. S. *J. Chem. Soc. A* **1969**, 1963–1972.
(17) (a) Rhodes, L. F.; Zubkowski, J. D.; Folting, K.; Huffman, J. C.; Caulton, K. G. *Inorg. Chem.* **1982**, *21*, 4185–4192. (b) Rhodes, L. F.; Huffman, J. C.; Caulton, K. G. *J. Am. Chem. Soc.* **1983**, *105*, 5137–5138.
(18) (a) Allison, J. D.; Cameron, C. J.; Wild, R. A.; Walton, R. A. *J. Organomet. Chem.* **1981**, *218*, C62–C66. (b) Allison, J. D.; Walton, R. A. *J. Chem. Soc., Chem. Commun.* **1983**, 401–402.
(19) (a) Douglas, P. G.; Shaw, B. L. *J. Chem. Soc. A* **1970**, 334–338. (b) Douglas, P. G.; Shaw, B. L. *Inorg. Synth.* **1978**, *17*, 64–66.
(20) (a) Carmona-Guzman, E.; Wilkinson, G. *J. Chem. Soc., Dalton Trans.* **1977**, 1716–1721. (b) Chiu, K. W.; Jones, R. A.; Wilkinson, G.; Galas, A. M. R.; Hursthouse, M. B.; Malik, K. M. A. *Ibid.* **1981**, 1204–1211.
(21) (a) Crabtree, R. H.; Hlatky, G. G. *J. Organomet. Chem.* **1982**, *238*, C21–C23. (b) Crabtree, R. H.; Hlatky, G. G.; Parnell, C. A.; Segmüller, B. F.; Uriarte, R. *Inorg. Chem.*, in press.
(22) Green, M. A.; Huffman, J. C.; Caulton, K. G. *J. Am. Chem. Soc.* **1982**, *104*, 2319–2320.
(23) Green, M. L. H.; McCleverty, J. A.; Pratt, L.; Wilkinson, G. *J. Chem. Soc.* **1961**, 4854–4859.

Table II. Fractional Coordinates and Isotropic Thermal Parameters for $[Os(NCMe)_3(PMe_2Ph)_3](PF_6)_2 \cdot CH_2Cl_2$

	10^4x	10^4y	10^4z	$10B_{iso}$, Å^2
Os(1)	2369.1 (2)	1934.4 (3)	3209.7 (4)	11
N(2)	2156 (4)	3382 (7)	3867 (8)	15
C(3)	1979 (5)	4231 (9)	4065 (9)	17
C(4)	1734 (5)	5275 (10)	4310 (10)	23
N(5)	1798 (4)	3018 (7)	1341 (8)	19
C(6)	1533 (5)	3698 (9)	313 (10)	20
C(7)	1185 (5)	4535 (10)	−1034 (10)	26
N(8)	3194 (4)	3142 (7)	2270 (8)	18
C(9)	3669 (5)	3748 (9)	1813 (10)	21
C(10)	4296 (5)	4496 (11)	1204 (12)	29
P(11)	2585 (1)	546 (2)	2137 (2)	16
C(12)	2417 (5)	−1174 (9)	3042 (10)	21
C(13)	2096 (5)	854 (10)	416 (10)	24
C(14)	3465 (5)	665 (9)	1615 (9)	18
C(15)	3669 (5)	1732 (10)	433 (10)	22
C(16)	4341 (5)	1872 (10)	27 (11)	27
C(17)	4807 (5)	965 (11)	815 (11)	28
C(18)	4605 (5)	−103 (10)	1962 (11)	27
C(19)	3931 (5)	−244 (10)	2353 (10)	21
P(20)	1372 (1)	785 (2)	4149 (3)	17
C(21)	747 (5)	482 (11)	2859 (12)	28
C(22)	1392 (5)	−798 (10)	5582 (11)	25
C(23)	865 (4)	1664 (9)	4856 (11)	20
C(24)	495 (5)	2667 (10)	3911 (12)	26
C(25)	127 (5)	3385 (11)	4396 (13)	33
C(26)	124 (5)	3081 (11)	5849 (14)	33
C(27)	496 (5)	2081 (11)	6806 (13)	32
C(28)	865 (5)	1373 (10)	6325 (11)	24
P(29)	3050 (1)	1044 (2)	5308 (2)	14
C(30)	3286 (5)	−612 (9)	5991 (10)	22
C(31)	2726 (5)	1139 (10)	6892 (10)	21
C(32)	3894 (4)	1863 (8)	5254 (9)	15
C(33)	4032 (5)	2787 (9)	5837 (10)	21
C(34)	4665 (5)	3422 (10)	5768 (11)	27
C(35)	5168 (5)	3176 (11)	5057 (11)	29
C(36)	5044 (5)	2287 (10)	4452 (11)	26
C(37)	4402 (5)	1631 (10)	4535 (10)	22
Cl(38)	6619 (2)	3754 (3)	−2560 (3)	35
C(39)	7058 (6)	3238 (12)	−865 (12)	37
Cl(40)	6810 (2)	1675 (3)	188 (3)	51
P(41)	6892 (1)	4587 (2)	2591 (3)	21
F(42)	6225 (3)	5394 (6)	2228 (6)	34
F(43)	7559 (3)	3776 (6)	2975 (7)	35
F(44)	7336 (4)	5715 (7)	2857 (8)	43
F(45)	7058 (3)	5206 (6)	954 (6)	36
F(46)	6730 (3)	3946 (9)	4220 (6)	54
F(47)	6436 (4)	3477 (6)	2280 (8)	43
P(48)	808 (2)	7453 (4)	221 (3)	37
F(49)	435 (6)	7042 (12)	−995 (11)	101
F(50)	1178 (5)	7828 (7)	1458 (8)	67
F(51)	302 (8)	6679 (24)	1194 (20)	218
F(52)	1272 (6)	6331 (11)	655 (12)	95
F(53)	421 (9)	8669 (17)	−239 (18)	166
F(54)	1291 (11)	8349 (16)	−814 (16)	171

in moderate gas evolution. At 25 °C this continues for 45–60 min with no visible precipitate. Addition of Et_2O causes prompt precipitation of a colorless solid. The ^{31}P NMR spectrum of this compound contains a singlet at −36.89 ppm. In addition to P–Ph and P–Me (18 H) resonances, the ^1H NMR spectrum contains a singlet (9 H) at 2.32 ppm, attributed to CH_3CN ligands. These are also evident as two $\nu(C{\equiv}N)$ bands in the infrared spectrum. There is no evidence of metal-bound hydride anywhere in the ^1H NMR spectrum. These data are consistent with the formulation *fac*-$Os(PMe_2Ph)_3(CH_3CN)_3^{2+}$, an 18-electron dication. We also found that treatment of $OsH_4(PMe_2Ph)_3$ with Ph_3CPF_6 (in CH_2Cl_2/CH_3CN) yielded this same complex. In view of the simplicity of the NMR spectra, we sought crystallographic verification of the proposed structure. Suitable crystals (from a Ph_3CPF_6 preparation) were obtained by cooling a solution of the compound in a mixture of CH_2Cl_2 and CH_3CN. The resulting structure corroborated the process shown in eq 2 (P ≡ PMe_2Ph). During the course of this work Crabtree and co-workers reported

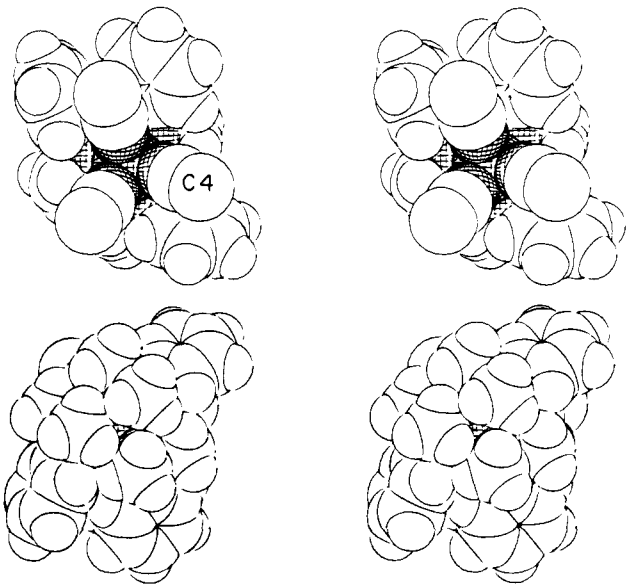

Figure 2. Space-filling model stereodrawings of *fac*-$Os(NCMe)_3(PMe_2Ph)_3^{2+}$ from two perspectives. Upper: three MeCN ligands project toward viewer (methyl hydrogens not shown). Lower: three PMe_2Ph ligands project toward viewer.

Table III. Bond Distances (Å) and Angles (deg) for $[Os(NCMe)_3(PMe_2Ph)_3](PF_6)_2 \cdot CH_2Cl_2$

Distances			
Os–P(11)	2.334 (2)	N(2)–C(3)	1.150 (11)
Os–P(20)	2.329 (2)	N(5)–C(6)	1.139 (12)
Os–P(29)	2.318 (2)	N(8)–C(9)	1.137 (12)
Os–N(2)	2.096 (8)	C(3)–C(4)	1.439 (13)
Os–N(5)	2.097 (8)	C(6)–C(7)	1.473 (14)
Os–N(8)	2.081 (8)	C(9)–C(10)	1.479 (13)
Angles			
P(11)–Os–P(20)	93.3 (1)	P(29)–Os–N(8)	89.8 (2)
P(11)–Os–P(29)	98.3 (1)	N(2)–Os–N(5)	83.1 (3)
P(20)–Os–P(29)	94.7 (1)	N(2)–Os–N(8)	85.2 (3)
P(11)–Os–N(2)	171.6 (2)	N(5)–Os–N(8)	85.0 (3)
P(11)–Os–N(5)	89.3 (2)	Os(1)–N(2)–C(3)	170.7 (7)
P(11)–Os–N(8)	90.6 (2)	Os(1)–N(5)–C(6)	173.5 (8)
P(20)–Os–N(2)	90.3 (2)	Os(1)–N(8)–C(9)	175.9 (8)
P(20)–Os–N(5)	89.9 (2)	N(2)–C(3)–C(4)	178.1 (10)
P(20)–Os–N(8)	173.5 (2)	N(5)–C(6)–C(7)	177.8 (10)
P(29)–Os–N(2)	89.0 (2)	N(8)–C(9)–C(10)	177.8 (11)
P(29)–Os–N(5)	170.9 (2)		

their observation of this same acidolysis reaction;[21b] our results are in agreement with theirs.

$$OsH_4P_3 + 2H^+ \text{ or } 2Ph_3C^+ \xrightarrow[CH_2Cl_2]{CH_3CN} \textit{fac}\text{-}OsP_3(CH_3CN)_3^{2+} \quad (2)$$

Structure of $[fac\text{-}Os(PMe_2Ph)_3(CH_3CN)_3](PF_6)_2$. The X-ray diffraction study confirms (Tables I–III and Figures 1 and 2) the facial octahedral geometry indicated by the ^1H and ^{31}P NMR data and the C≡N infrared data. The colorless crystals yield a lattice with 1 mol of CH_2Cl_2 for each osmium, a result that was quantitatively confirmed by ^1H NMR spectroscopy. The three Os–N distances are identical to within 2σ, while the three Os–P distances differ by less than 5σ. Among the acetonitrile ligands, C≡N and C–CH_3 bond lengths are identical to within $1\text{–}3\sigma$, and the N≡C–C angles differ insignificantly from 180°. Noteworthy is the manner in which the *fac*-MX_3Y_3 unit deviates from orthogonality in a system where the X ligands are bulky and the Y ligands are slender. The P–Os–P angles predictably increase from 3 to 8° above 90°, while the N–Os–N angles decrease from 5 to 7° below 90°. However, these distortions occur in a manner such that all cis N–Os–P angles remain at 90.0 ± 1.0°. The trigonal distortions thus occur so as to avoid any decrease in cis N···P distances.

Mechanism of Acidolysis. In view of the multistep nature of the conversion of $OsH_4(PMe_2Ph)_3$ to *fac*-$Os(PMe_2Ph)_3$-

$(CH_3CN)_3^{2+}$, we sought information on the sequence of protonation (twice), H_2 elimination (three times), and CH_3CN addition (three times) steps. The course of the acidolysis process is most conveniently studied via ^{31}P NMR. Hence, OsH_4P_3 (^{31}P = −28.8 ppm) was dissolved in CH_2Cl_2/CH_3CN (50:50) in an NMR tube, and excess $HBF_4 \cdot OEt_2$ was added to start the reaction. Initially one observes a singlet resonance at −33.96 ppm, which decays over 20–30 min at room temperature, giving rise to another singlet at −33.80 ppm. This signal also decays over 10–20 min, with a concurrent growth of a singlet at −36.89 ppm, due to formation of *fac*-$OsP_3(CH_3CN)_3^{2+}$. To simplify the discussion of this process we first present a proposed mechanistic pathway (Scheme I). Although the overall conversion of **1** to **6** is portrayed as passing through a large number of intermediates, we have successfully obtained spectroscopic characterization of each numbered species. All contain 18 valence electrons but display varying stabilities and lifetimes. We now present conditions that allowed characterization of the individual species.

Scheme I

$$\underset{\mathbf{1}}{OsH_4P_3} + H^+ \xrightarrow[CH_2Cl_2]{} \underset{\mathbf{2}}{OsH_5P_3^+}$$

$$\mathbf{2} \xrightarrow[-H_2]{CH_3CN} \underset{\mathbf{3}}{OsH_3P_3(CH_3CN)^+}$$

$$\mathbf{3} \xrightarrow[-H_2]{CH_3CN} \underset{\mathbf{4}}{OsHP_3(CH_3CN)_2^+}$$

$$\mathbf{4} + H^+ \xrightarrow[-H_2]{CH_3CN} \underset{\mathbf{5}}{mer\text{-}OsP_3(CH_3CN)_3^{2+}}$$

$$\mathbf{5} \rightarrow \underset{\mathbf{6}}{fac\text{-}OsP_3(CH_3CN)_3^{2+}}$$

Protonation of OsH_4P_3 to $[OsH_5(PMe_2Ph)_3]BF_4$ (2). Douglas and Shaw[19] have presented conductometric evidence for the simple protonation of OsH_4P_3 with HCl and CF_3CO_2H, but the presence of $OsH_5P_3^+$ was not spectroscopically verified. Since subsequent chemistry (in Scheme I) seemed to involve CH_3CN, we carried out the protonation of OsH_4P_3 in neat CH_2Cl_2 (eq 3). The ^{31}P

$$OsH_4P_3 + H^+ \xrightarrow[CH_2Cl_2]{} OsH_5P_3^+ \qquad (3)$$

spectrum showed the transient singlet at −33.96 ppm detected previously in the experiment with excess acid, but it now showed no decay (i.e., in the absence of CH_3CN). Selective coupling to metal-bound hydrides did lead to a broadened ^{31}P NMR signal, but the coupling was too small to resolve. At −60 °C, the $^{31}P\{^1H\}$ spectrum showed a very broad signal, indicating a fluxional process was slowed but not frozen out. The ^1H NMR spectrum (CD_2Cl_2, 220 MHz) exhibited, in addition to P–Me and P–Ph resonances, a hydride signal at −7.02 ppm. At lower operating frequency (60 MHz) this was resolvable into a quartet with $^2J_{PH}$ = 4 Hz, consistent with an $OsP_3H_x^+$ formulation. Theoretically the value of x could be determined by integration of the ^1H NMR spectrum, but we have observed inaccuracies in the integration of compounds like these.[17b] To show that x = 5, OsH_4P_3 was protonated with excess $HBF_4 \cdot OEt_2$, and formation of $OsP_3H_x^+$ (**2**) was confirmed by ^{31}P NMR spectroscopy. Excess NEt_3 was then added and another spectrum recorded, showing complete regeneration of OsH_4P_3. This was taken as evidence of simple protonation and thus establishes **2** as $OsH_5P_3^+$. Interestingly, if limiting quantities of acid are employed, both OsH_4P_3 and $OsH_5P_3^+$ are observed via ^{31}P NMR spectroscopy, indicating that this acid–base conjugate pair does not undergo rapid exchange under these conditions.

Spectral Characterization of $[OsH_3(PMe_2Ph)_3(CH_3CN)](BF_4)$ (3). Considering stoichiometry alone, the production of **3** (Scheme I) requires only 1 equiv each of acid and CH_3CN. Hence, the reaction (eq 4) was carried out with 1 equiv of acid and only a

$$\underset{\mathbf{1}}{OsH_4P_3} + H^+ + CH_3CN \xrightarrow[CH_2Cl_2]{} \underset{\mathbf{3}}{OsH_3P_3(CH_3CN)^+} + H_2 \qquad (4)$$

slight excess of CH_3CN. Subsequent spectra confirmed that further reaction of **3** was negligible with this stoichiometry and at 25 °C.

At 25 °C the $^{31}P\{^1H\}$ NMR spectrum of **3** displays a singet at −33.80 ppm. Due to near overlap with the resonance of **2** (−33.96 ppm) a selectively hydride-coupled spectrum could not be obtained. Moreover, the ^1H NMR spectrum indicated the coupling constant ($^2J_{PH}$) was very small (vide infra) and probably not resolvable in the ^{31}P NMR spectrum. The ^1H NMR spectrum showed the aforementioned resonances for **2**, as well as free CH_3CN (1.97 ppm) and Et_2O (3.49 (q), 1.15 (t)) from the $HBF_4 \cdot OEt_2$. The spectrum of **3** contains P–Ph and P–Me resonances at 7.51 and 1.83 ppm, an Os–H quartet ($^2J_{P-H}$ = 4 Hz) at −10.02 ppm, and a singlet at 2.31 ppm for the CH_3CN ligand. It should be noted that the facile fluxional process (rapid even at −35 °C) in **3** is entirely consistent with its formulation as a seven-coordinate species. For example, $K^+OsH_3(PMe_2Ph)_3^-$ and OsH_4P_3 (**1**) are both 18-electron compounds with multiple hydride ligands; the former (six-coordinate) is conformationally rigid at 25 °C[24] while the latter is stereochemically nonrigid.

Synthesis of $[OsH(PMe_2Ph)_3(CH_3CN)_2](BF_4)$ (4). It is interesting to note that under conditions of excess acid and CH_3CN, compound **4** (Scheme I) is never observed during the ^{31}P NMR monitoring of the conversion of **1** to **6**. Since **4** is a monocation and a likely intermediate in the process, we carried out the reaction shown in eq 5 with 1 equiv of $HBF_4 \cdot OEt_2$ but a large excess of

$$OsH_4P_3 + H^+ \xrightarrow[CH_2Cl_2]{CH_3CN} \underset{\mathbf{4}}{OsHP_3(CH_3CN)_2^+} \qquad (5)$$

CH_3CN; under these conditions, the reaction is observed to proceed through species **2** and **3** (^{31}P NMR) but never reaches compound **6**. The product (**4**) exhibits an A_2B pattern with a doublet at −26.05 ppm and a triplet at −31.40 ppm ($^2J_{P-P}$ = 21 Hz). Selective coupling to the hydride ligand converts the doublet to a doublet of doublets ($^2J_{P-H}$ = 16 Hz) and the triplet to a virtual quartet in which $^2J_{P-H} \approx {}^2J_{P-P}$. The ^1H NMR spectrum shows P–Ph at 7.2–7.6 ppm, P–Me at 1.59 (12 H) and 1.37 ppm (6 H), CH_3CN at 2.51 and 1.95 ppm, and Os–H at −16.60 ppm (virtual quartet, J(apparent) ≈ 15 Hz). Although the A_2B phosphine pattern could be consistent with either a facial or meridional arrangement of these nuclei, the similar (and somewhat small) P–H coupling constants indicated the hydride was cis to all three phosphines. This observation together with the presence of two inequivalent CH_3CN ligands requires the mer,cis structure as shown.

4, L = CH_3CN

These data are also consistent with data for *mer,cis*-$RuH(ttp)L_2^+$, in which ttp is $PhP(CH_2CH_2CH_2PPh_2)_2$ and L = CH_3CN.[25] This compound exhibits a virtual quartet for the hydride with $J_{P_1-H} \approx J_{P_2-H}$ = 19 Hz. Further, *mer,cis*-$RuH(PPh_3)_3(CH_3CN)_2^+$ has been prepared from $RuH_2(PPh_3)_4$ and Ph_3CPF_6 in CH_3CN.[26] We suspected that OsH_4P_3 could likewise be converted to **4** with 1 equiv of Ph_3CPF_6; indeed the reaction proceeds cleanly in this manner, as verified by ^{31}P NMR spectroscopy.

Crabtree has shown that cationic hydrides of iridium with weakly bound ligands L ($IrH_2L_2P_2^+$) are active in a wide range of interesting transformations of small organics.[14] However, no such activity was exhibited by **6** or by $WH_2(CH_3CN)_3P_3^{2+}$, ostensibly because the CH_3CN ligand is too tightly bound.[21] In compound **4**, however, one CH_3CN is trans to a hydride, and previous workers have observed facile dissociation under such

(24) Green, M. A.; Caulton, K. G., unpublished observations.
(25) (a) Mazanec, T. J.; Letts, J. B.; Meek, D. W. *J. Chem. Soc., Chem. Commun.* **1982**, 356–358. (b) Letts, J. B.; Mazanec, T. J.; Meek, D. W. *J. Am. Chem. Soc.* **1982**, *104*, 3898–3905. (c) Letts, J. B.; Mazanec, T. J.; Meek, D. W. *Organometallics*, **1983**, *2*, 695–704.
(26) Sanders, J. R. *J. Chem. Soc., Dalton Trans.* **1973**, 743–747.

circumstances.[25,27] Indeed, addition of CH_3CN to an NMR solution of **4** (CD_2Cl_2) results (within 5 min) in a decrease in the resonance at 2.51 ppm with a concurrent growth of a signal for free CH_3CN at 1.97 ppm, indicating facile exchange. This suggests that **4** may be reactive with other organic nucleophiles.

Finally, we sought evidence that **4** truly lies on the pathway to **6**. In an NMR tube, **4** (prepared with 1 equiv of H^+) was dissolved in a mixture of CD_2Cl_2 and CD_3CN and a spectrum recorded. Addition of a second equivalent of $HBF_4 \cdot OEt_2$ caused immediate disappearance of **4** (^{31}P NMR), ultimately giving **6**, as verified by ^{31}P and ^1H NMR spectroscopy.

Spectral Observation of 5. When the acidification of **4** was carried out (as above) and monitored via ^{31}P NMR, we observed an intermediate compound **5** with a lifetime of only a few minutes at room temperature. Like compound **4**, **5** is never observed when OsH_4P_3 is converted to **6** with excess acid. Compound **5** exhibits an A_2B pattern in the ^{31}P NMR spectrum (distinct from that of **4**) with a doublet at −30.5 ppm and a triplet at −40.8 ppm ($^2J_{P-P}$ = 17 Hz). Unfortunately, this compound is too short-lived for further spectroscopic characterization. Protonation of **4** and loss of H_2 would presumably occur via two steps (eq 6 and 7). We

$$\underset{\mathbf{4}}{OsHP_3L_2^+} + H^+ \rightarrow OsH_2P_3L_2^{2+} \quad (6)$$

$$OsH_2P_3L_2^{2+} + L \xrightarrow{-H_2} \underset{\mathbf{5}}{mer\text{-}OsP_3L_3^{2+}} \quad (7)$$

disfavor the identification of **5** as $OsH_2P_3L_2^{2+}$ because the latter is seven-coordinate and would probably show equivalent phosphines due to rapid fluxionality. Rather, we suspect **5** is the meridional isomer of $OsP_3(CH_3CN)_3^{2+}$, which rapidly isomerizes to facial **6**. It would appear that the conversions **4** → **5** and **5** → **6** proceed at comparable rates (with the former slightly faster) under the conditions employed, since **5** is only observed when large quantities of **4** are initially present.

General Considerations

The present work exemplifies several interesting points related to polyhydride reaction patterns. First, it has been noted that although cationic dihydrides are somewhat common,[14,28] cationic $MH_xL_y^+$ species with $x \geq 3$ are relatively rare.[21b] In this work both **2** and **3** are observed, but both readily lose H_2, particularly in the presence of potential ligands (CH_3CN). This reductive elimination is not unexpected in high-valent, highly coordinatively saturated compounds such as these. However, the fact that they proceed slowly enough to observe is a surprising consequence of the kinetic inertness of third-row transition metals. Further, the identification of **2** verifies that when metal d electrons are available, protonolysis seems to occur via a stepwise protonation–elimination sequence. The difference between this pathway and reaction with Ph_3C^+ is that the latter appears to proceed via hydride abstraction (possibly via an electron transfer/H atom transfer sequence[18,29]). Thus, while acidolysis converts **1** to **3** via **2**, Ph_3C^+ is thought to convert **1** directly to **3**, provided CH_3CN is present. If **1** is treated with Ph_3C^+ in neat CH_2Cl_2, the result is a complex mixture of uncharacterized products.

The acidolysis of **1** to **6** involves two protonation steps and three H_2 eliminations. Protonation of cationic $Rh(diphos)_2^+$ has been reported;[30] similarly, $(arene)Mo(PR_3)_3$ can be protonated once in dilute acid and twice in concentrated acid (eq 8).[31] In the

$$(C_6H_6)MoP_3 \xrightarrow{H^+} (C_6H_6)MoP_3H^+ \xrightarrow{H^+} (C_6H_6)MoP_3H_2^{2+} \quad (8)$$

present system this sequence is clearly not operative. As shown in Scheme I, we observe single protonation to $OsH_5P_3^+$ (**2**), which must then lose two molecules of H_2 and gain two CH_3CN ligands before the second protonation occurs. The ready isolation of monocation **4** provides strong evidence for this. As such, we concur with the postulate that the σ-donor CH_3CN ligands in **4** are required to render the cationic osmium center basic enough for a second protonation.[21b]

A final point concerns the conversions **2** → **3** and **3** → **4**. As shown in Scheme I, both are thought to involve reaction with CH_3CN. Again, this is verified in the first case by the long lifetime of **2** in neat CH_2Cl_2. While it appears that incoming ligand serves to induce H_2 elimination, the exact mechanism of this transformation is unclear. Since this is a reaction of fundamental importance in polyhydride chemistry, further mechanistic definition was desirable. We envisioned two likely pathways and chose to study the conversion of **2** to **3** since **2** is more readily available in pure form. One possible mechanism would be a S_N2 process, first order in CH_3CN, proceeding through the transition state $[OsH_5P_3(CH_3CN)^+]^\ddagger$ of unspecified structure and bonding.

The second mechanistic alternative is depicted in eq 9 and

$$OsP_3H_xL_y^+ \underset{k_{-1}}{\overset{k_1}{\rightleftharpoons}} H_2 + [OsP_3H_{x-2}L_y^+] \xrightarrow[k_2]{L} OsP_3H_{x-2}L_{y+1}^+ \quad (9)$$

2, $x = 5$, $y = 0$
3, $x = 3$, $y = 1$

involves an equilibrium H_2 loss to give a reduced osmium compound. This 16-electron transient is expected to be very reactive and the equilibrium should lie well to the left. Upon addition of L, the reduced species is trapped rapidly to give the resulting product. Any ability of CH_2Cl_2 to stabilize the intermediate is expected to have little effect on the process since CH_3CN should displace CH_2Cl_2 very readily.[32]

We have employed two probes to distinguish the mechanistic possibilities. Specifically, the S_N2 process should exhibit a rate dependence on the concentrations of both **2** and CH_3CN, or overall second-order behavior. The mechanism in eq 9 should follow the rate equation in eq 10, derived by applying the steady-state ap-

$$-\frac{d[\mathbf{2}]}{dt} = k_1[\mathbf{2}]\left[1 - \frac{k_{-1}[H_2]}{k_2[L] + k_{-1}[H_2]}\right] \quad (10)$$

proximation to the 16-electron intermediate. In the limiting case where $k_2[L] \gg k_{-1}[H_2]$, eq 10 reduces to eq 11, indicating an

$$-d[\mathbf{2}]/dt = k_1[\mathbf{2}] \quad (11)$$

overall first-order process which is independent of CH_3CN concentration. Thus, the process in eq 9 reduces to a two-step reaction in which the first step is rate limiting. The above assumption is reasonable since the reaction is carried out under a N_2 atmosphere at ambient pressure. Thus the concentration of H_2 in solution is considerably lower than that of CH_3CN.

The kinetic order of the reaction (**2** with CH_3CN) with respect to CH_3CN was determined at 20 °C. This was conveniently achieved by monitoring the disappearance of **2** (as well as the appearance of **3** and **6**) via ^{31}P NMR spectroscopy. Rates were

Table IV. Kinetics of Reaction of **2** with CH_3CN[a]

solution	$[CH_3CN]$, M	k_{obsd},[b] s^{-1}
1	0.69	$(2.8 \pm 0.2) \times 10^{-4}$
2	3.5	$(3.1 \pm 0.2) \times 10^{-4}$

[a] Both solutions 0.093 M in **2**, CH_2Cl_2 solvent, 20 °C. [b] Determined from the least-squares slope of plots of $\ln [(2)_0/(2)_t]$ vs. time. Errors are estimated uncertainties of slopes.

(27) Schrock, R. R.; Osborn, J. A. *J. Am. Chem. Soc.* **1976**, *98*, 2134–2143.
(28) (a) Schrock, R. R.; Osborn, J. A. *J. Am. Chem. Soc.* **1976**, *98*, 2143–2147. (b) Schrock, R. R.; Osborn, J. A. *Ibid.* **1976**, *98*, 4450–4455. (c) Shapley, J. R.; Schrock, R. R.; Osborn, J. A. *Ibid.* **1969**, *91*, 2816–2817. (d) Schrock, R. R.; Osborn, J. A. *Ibid.* **1971**, *93*, 2397–2407.
(29) Hayes, J. C.; Cooper, N. J. *J. Am. Chem. Soc.* **1982**, *104*, 5570–5572.
(30) Halpern, J.; Riley, D. P.; Chan, A. S. C.; Pluth, J. J. *J. Am. Chem. Soc.* **1977**, *99*, 8055–8057.
(31) Green, M. L. H.; Mitchard, L. C.; Silverthorn, W. E. *J. Chem. Soc., Dalton Trans.* **1974**, 1361–1363.
(32) Crabtree, R. H.; Faller, J. W.; Mellea, M. F.; Quirk, J. M. *Organometallics* **1982**, *1*, 1361–1366.

obtained with a 4.5- and 23-fold excess of CH_3CN (vs. **2**), and the resulting values of k_{obsd} are given in Table IV. Two observations are noteworthy. First, both reactions followed first-order kinetics over 2–3 half-lives, even though the first reaction did not involve pseudo-first-order conditions; i.e., there was not a large excess of CH_3CN. Second, the two rates are equal to within ca. 10%; a first-order dependence on CH_3CN would have resulted in a 5- to 6-fold difference in k_{obsd} for the two reactions. We assume that the small difference reflects the accuracy of the method and consider the reaction rate to be independent of CH_3CN concentration.

It is possible to augment the kinetic evidence for the preequilibrium mechanism in eq 9 by direct detection of the equilibrium itself. This equilibrium, if it exists, provides a mechanism for exchange of hydride ligands in $OsH_5P_3^+$ with D_2, without requiring the presence of CH_3CN. Thus, OsH_4P_3 (**1**) was protonated with $HBF_4{\cdot}OEt_2$ (2.5 equiv) in CH_2Cl_2 and stirred under 400 psi of D_2 for 1 h. At that time excess NEt_3 was added and the resulting **1** analyzed for deuterium content. The ^2D NMR spectrum exhibited a signal at ca. −9.0 ppm, indicative of Os–D. There was no evidence of deuterium in the phosphine ligands. The proton spectrum of **1** was then integrated to determine the approximate extent of D incorporation; this indicated a 70% loss of Os–H in favor of Os–D. Thus, both the kinetics and the deuterium labeling study favor eq 9 as the pathway from **2** to **3**.[34] Acetonitrile thus functions to trap the product of a dihydrogen reductive elimination equilibrium and does not actively displace H_2.

Summary

The conversion of OsH_4P_3 (**1**) to *fac*-$OsP_3(CH_3CN)_3^{2+}$ (**6**) is a multistep process involving several intermediates. This multiple loss of hydride ligands (as H_2) appears to be a general reaction of polyhydrides, induced by acidolysis, hydride abstraction, or oxidation. Using combinations of limiting reagent concentrations and/or low temperatures we have been able to isolate or spectroscopically observe many of these intermediate species. From these studies several characteristics of osmium polyhydrides have been identified. First, although the overall conversion **1** → **6** involves two protonations, these occur in separated (i.e., not consecutive) steps. The second protonation is only observed after formation of $OsHP_3(CH_3CN)_2^+$, apparently facilitated by the electron-donating ability of CH_3CN. Also, osmium compounds with coordination number greater than six show a marked tendency toward fluxionality while six-coordinate complexes are rigid. Such rigidity may account for the stereospecificity of the acidolysis of **4** (mer,cis) to **5** (mer) rather than directly to **6** (fac). Further, the reactions observed here show a tendency toward achieving octahedral coordination (within the constraints of the 18-electron rule) when suitable reagent stoichiometries are provided. Finally, the favorable (i.e., sluggish) kinetics of this particular system have allowed elucidation of several reactivity patterns of polyhydrides. These may serve as an acceptable model for acidolysis reactions of more labile systems, as well as for fundamental polyhydride transformations other than acidolysis.

Experimental Section

All manipulations were carried out under a N_2 atmosphere by using standard Schlenk techniques. Solid transfers were accomplished in a Vacuum Atmospheres Corp. glovebox. Methylene chloride (Aldrich) and acetonitrile (Aldrich) were distilled (under N_2) from P_2O_5 and CaH_2, respectively, and stored over Linde 4A molecular sieves. Ph_3CPF_6 (Aldrich) was recrystallized from CH_2Cl_2 prior to use and stored under N_2. $HBF_4{\cdot}OEt_2$ (Aldrich) was used as received and transferred under a N_2 purge. $OsH_4(PMe_2Ph)_3$ was synthesized according to the literature method,[19a] starting from OsO_4 (Johnson-Matthey).

^{31}P NMR spectra were obtained on a Varian XL-100 instrument (FT, 40.5 MHz). Negative chemical shifts are upfield from external 85% H_3PO_4. ^1H NMR spectra were obtained on a Varian instrument (CW, 220 MHz). IR spectra were recorded on a Perkin-Elmer 283 instrument.

Synthesis of [*fac*-Os(PMe$_2$Ph)$_3$(CH$_3$CN)$_3$](BF$_4$)$_2$ (6). In the glovebox, 200 mg (0.33 mmol) of OsH_4P_3 was weighed into a Schlenk flask. On a Schlenk line, 5 mL each of CH_3CN and CH_2Cl_2 was added. Similarly, 75 μL (0.12 g, 0.74 mmol) of $HBF_4{\cdot}OEt_2$ was added, and the solution was stirred at room temperature. When gas evolution had ceased (ca. 20 min), 20 mL of diethyl ether was added slowly. The resulting colorless solid was filtered and washed with ether. IR (KBr): ν(CN) 2292 (w), 2310 (w) cm^{-1}, $^{31}P\{^1H\}$ NMR (CD_3CN): −36.89 (s) ppm. ^1H NMR (CD_3CN) δ 7.26 (m, P–Ph), 2.32 (s, 9 H, CH_3CN), 2.05 (d, 18 H, P–Me, $^2J_{PH}$ = 8 Hz). When **6** was prepared with CD_3CN, the singlet at δ 2.32 was absent.

Alternatively, **6** was prepared as the PF_6^- salt from Ph_3CPF_6. In a Schlenk flask was prepared a solution of 300 mg (0.8 mmol) of Ph_3CPF_6 in 10 mL of CH_3CN. A second solution of 250 mg (0.41 mmol) of OsH_4P_3 in 8 mL each of CH_2Cl_2 and CH_3CN was added slowly via an addition funnel. Addition was stopped when the yellow color of Ph_3CPF_6 disappeared. The resulting solution was stripped in vacuo and the residue washed with 10 mL of toluene (to remove Ph_3CH and unreacted OsH_4P_3). Crystals for X-ray diffraction were obtained by slowly cooling (−20 °C) a solution of **6** (PF_6^-) in 90:10 CH_2Cl_2/CH_3CN. The compound prepared this way had spectral identical with that of the acidolysis product but also showed a PF_6^- resonance (−144.5 ppm, septet, J_{P-F} = 708 Hz).

X-ray Crystallography. A suitable sample was cleaved from a larger crystal and transferred to the goniostat by using standard inert-atmosphere techniques. A systematic search of a limited hemisphere of reciprocal space revealed no systematic absences or symmetry, indicating a triclinic lattice. Parameters of the data collection[33] are shown in Table I. No absorption correction was applied. The structure was solved by Patterson and Fourier techniques, followed by full-matrix refinement. A stoichiometric solvent (CH_2Cl_2) of crystallization was present. A difference Fourier phased on all non-hydrogen atoms clearly revealed hydrogen atoms with the exception of those on the MeCN ligands. Final cycles included hydrogens (except those of MeCN) as fixed-atom contributors in idealized (C–H distance = 0.95 Å) positions. A final difference Fourier indicated hydrogen positions for one of the MeCN ligands and was otherwise featureless.

The results of the structural study are shown in Tables II and III and Figures 1 and 2. Further details (including peripheral ligand, PF_6^-, and CH_2Cl_2 parameters) are available as Supplementary Material.

Synthesis of [*mer*,*cis*-OsH(PMe$_2$Ph)$_3$(CH$_3$CN)$_2$](BF$_4$) (4). In the glovebox, 200 mg (0.33 mmol) of OsH_4P_3 was added to a Schlenk flask. On the Schlenk line, 5 mL each of CH_3CN and CH_2Cl_2 was added, followed by 35 μL (58 mg, 0.36 mmol) of $HBF_4{\cdot}OEt_2$. The solution was stirred at room temperature for 45 min and then stripped to dryness in vacuo. The residue was washed with 10 mL of ether, yielding a colorless oily solid. Although the solid was greater than 90% pure (^{31}P NMR), it was difficult to isolate **4** without traces of **3** and **6** present. $^{31}P\{^1H\}$ NMR (CD_2Cl_2): −26.05 (d), −31.40 (t) (J_{PP} = 21 Hz) ppm, ^{31}P NMR (selectively coupled to hydrides) (CD_2Cl_2): −26.05 (d of d, J_{PH} = 16 Hz), −31.40 (virtual q, apparent J_{P-H} = 16 Hz) ppm. ^1H NMR: δ 7.2–7.6 (m, P–Ph), 2.51 (s, 3 H, CH_3CN trans to H), 1.95 (s, 3 H, CH_3CN), 1.59 (d, 12 H, P–Me, J_{PH} = 11 Hz), 1.37 (d, 6 H, P–Me, J_{PH} = 9 Hz), −16.60 (virtual q, 1 H, Os–H, apparent J = 16 Hz). Addition of CD_3CN caused a decrease in the signal at 2.51 ppm, with evidence of free CH_3CN at 1.97 ppm. The resonance at 1.95 ppm was unaffected.

Spectral Observation of [OsH$_5$(PMe$_2$Ph)$_3$](BF$_4$) (2). OsH_4P_3 (100 mg, 0.16 mmol) was added to an NMR tube and dissolved in CD_2Cl_2. To this solution was added 20 μL (30 mg, 0.21 mmol) of $HBF_4{\cdot}OEt_2$. The resulting compound (formed quantitatively (^{31}P)) was stable in solution for hours. $^{31}P\{^1H\}$ NMR (CD_2Cl_2): −33.96 (s) ppm. Hydride coupling was not resolved but led to significant broadening of the observed singlet. ^1H NMR (CD_2Cl_2): δ 7.47 (m, P–Ph), 1.78 (d, P–Me, J_{PH} = 8 Hz), −7.02 (q, Os–H, J_{PH} = 4 Hz). Addition of excess NEt_3 to this solution resulted in regeneration of OsH_4P_3 (^{31}P = −28.80) with no phosphorus-containing byproducts.

Spectral Observation of [OsH$_3$(PMe$_2$Ph)$_3$(CH$_3$CN)](BF$_4$) (3). OsH_4P_3 (60 mg, 0.10 mmol) was added to an NMR tube and dissolved in CD_2Cl_2. To this solution was added 15 μL (25 mg, 0.15 mmol) of $HBF_4{\cdot}OEt_2$. The tube was immersed in a −78 °C slush bath, and 10 μL of CH_3CN was added. The sample was immediately inserted into the NMR probe cooled to −35 °C for a ^{31}P NMR spectrum. This showed overlapping singlets for **2** (−33.96 ppm) and **3** (−33.80 ppm). Subsequently ^1H NMR data were obtained at 25 °C. In addition to resonances

(33) Details of the data collection, processing, and refinement techniques are given in: Huffman, J. C.; Lewis, L. N.; Caulton, K. G. *Inorg. Chem.* **1980**, *19*, 2755.

(34) A referee has suggested that the available data are consistent with a preequilibrium in eq 9 (x = 5, y = 0) with dissociation of PMe_2Ph instead of H_2. We are less attracted to this possibility since PMe_2Ph, once dissociated, would probably not be competitive with the 23-fold excess of MeCN for recoordination to osmium; the predicted bis(phosphine) complexes were never observed.

of **2**, free CH_3CN (1.97 ppm), and Et_2O (3.49 (q), 1.15 (t)), the resonances for **3** were observed. ^1H NMR (CD_2Cl_2): δ 7.51 (m, P–Ph), 2.31 (s, CH_3CN), 1.63 (d, P–Me, J_{PH} = 8 Hz), −10.02 (q, Os–H, J_{PH} = 4 Hz).

Kinetic Studies. In the glovebox, 225 mg (0.37 mmol) of OsH_4P_3 was weighed and dissolved in 2.0 mL of CH_2Cl_2 (0.19 M). Under N_2 purge, 80 μL of $HBF_4{\cdot}OEt_2$ (0.82 mmol) was added. The excess was employed to ensure production of only **3** and **6** (singlets in ^{31}P); the A_2B pattern of **4** would be more difficult to integrate. The above solution was transferred to two NMR tubes (0.5 mL each). To the first was added 110 μL of a 4:1 CH_2Cl_2/CH_3CN solution (0.42 mmol of CH_3CN, 0.69 M), and the reaction was monitored via $^{31}P\{^1H\}$ NMR (20 °C). To the second tube was added 110 μL of neat CH_3CN (2.12 mmol of CH_3CN, 3.5 M), and the reaction was monitored similarly. Both reactions lasted 1–1.5 h, and spectra were recorded (15 s acquisition time) every 5–10 min. The rate of disappearance of **2** exhibited first-order behavior and the rate constant k_{obsd} ($\equiv k_1$, eq 9) was determined as the slope of a plot of ln $[(\mathbf{2})_0/(\mathbf{2})_t]$ vs. time; data are given in Table IV.

Acknowledgment. This work was supported by Dow Chemical Corp. and by the Bloomington Academic Computing System. The deuterium NMR spectra were obtained on an instrument funded in part by NSF Grant No. CHE-80-05004.

Registry No. 1, 24228-57-7; **2** (BF_4), 88703-91-7; **3** (BF_4), 88703-93-9; **4** (BF_4), 88703-95-1; **5**, 88764-07-2; **6** $(PF_6)_2{\cdot}CH_2Cl_2$, 88703-96-2; **6** $(PF_6)_2$, 88703-89-3; **6** $(BF_4)_2$, 88129-95-7; $HBF_4{\cdot}OEt_2$, 67969-82-8; Ph_3CPF_6, 437-17-2; CH_3CN, 75-05-8.

Supplementary Material Available: Anisotropic temperature factors, distances and angles within the PMe_2Ph, PF_6^-, and CH_2Cl_2 moieties, and observed and calculated structure factors for $[Os(NCMe)_3(PMe_2Ph)_3](PF_6)_2{\cdot}CH_2Cl_2$ (36 pages). Ordering information is given on any current masthead page.

Structural Phase Transitions in Dihalo(*N*,*N*′-disubstituted-diazabutadiene)nickel Complexes. Structures of Bis[dibromo(*N*,*N*′-di-*tert*-butyldiazabutadiene)nickel] and Dibromo(*N*,*N*′-di-*tert*-butyldiazabutadiene)nickel

Geoffrey B. Jameson,*† Hans Rudolf Oswald,‡ and Hans Rudolf Beer‡

Contribution from the Department of Chemistry, Georgetown University, Washington, DC 20057, and the Institute of Inorganic Chemistry, University of Zürich, 8057 Zürich, Switzerland.
Received April 25, 1983

Abstract: Violet tetrahedral complexes $NiX_2(dab)$ (X = Br, Cl; dab = *N*,*N*′-disubstituted-diazabutadienes) are formed when crystals of the yellow dimers $[NiX_2(dab)]_2$ are heated. The structural transformation when X = Br and dab = *N*,*N*′-di-*tert*-butyldiazabutadiene is irreversible but topotactic—single crystallinity is largely preserved in the transformation. The yellow complex has been found by single-crystal X-ray structure analysis to be a distorted trigonal-bipyramidal centrosymmetric dimer: Ni–Br(terminal) = 2.457 (1) Å, Ni–Br(bridging) = 2.497 (1) and 2.583 Å, Ni–N = 2.042 (4) and 2.039 (4) Å, Br(terminal)–Ni–Br(bridging, long) = 165.79 (3)° (defines the pseudotrigonal axis), Br(bridging)–Ni–Br(bridging) = 83.11 (3)°, N–Ni–N = 80.8 (2)°. The monomer (structural analysis of a sample separately prepared at ~130 °C) has tetrahedral D_{2h} symmetry: Ni–Br = 2.333 (2) and 2.343 (2) Å, Ni–N = 1.996 (7) and 2.002 (8) Å, Br–Ni–Br = 126.78 (6)°, N–Ni–N = 82.5 (3)°. The reaction mechanism involves cleavage of the long Ni–Br bond and concerted movement of $NiBr_2(dab)$ monomers with concomitant rearrangement to a tetrahedral D_{2d} system such that centrosymmetrically related Ni centers, formerly 3.806 Å separated, become separated by 9.893 Å and related by a 2_1 screw axis. Movements of the monomeric $NiBr_2(dab)$ units of about 10 Å are observed, while crystallinity is largely preserved. Relevant crystal and refinement data are as follows. For $[NiBr_2(dab)]_2$: space group C_{2h}^6–$C2/c$, a = 20.429 (5) Å, b = 7.156 (1) Å, c = 20.504 (5) Å, β = 98.50 (2)°, V = 2965 Å^3 at 22 °C, Z = 4 (dimers have $\bar{1}$ symmetry), ρ_{calcd} = 1.73, ρ_{obsd} = 1.72 (1) g/cm^3, 2560 reflections with $I > 3\sigma_I$ in the range $0.0246 < (\sin\theta)/\lambda < 0.7049$ Å^{-1} (graphite-monochromated Mo Kα radiation), R and R_w on F 0.039 and 0.047. For $NiBr_2(dab)$: space group C_{2h}^5–$P2_1/n$, a = 7.125 (3) Å, b = 19.717 (10) Å, c = 10.396 (5) Å, β = 90.91 (2)°, V = 1459 Å^3 at −150 °C, Z = 4, ρ_{calcd} = 1.67, ρ_{obsd} = 1.66 (1) g/cm^3 (based upon room-temperature cell constants), 2300 reflections in the range $0.0246 < (\sin\theta)/\lambda < 0.5734$ Å^{-1}, R and R_w on F^2 (all data including $F^2 < 0$ was used) 0.091 and 0.127, for the 1545 reflections with $I > 3\sigma_I$ R and R_w on F 0.055 and 0.062.

The evaluation of kinetic parameters for solid-state reactions and structural phase transitions is conventionally based on analogy to the theory for processes occurring in homogeneous solution for lack of any better formulation.[1] Thus, when free mobility of particles can no longer occur, when temperature exchange between the reacting species and solvent is not relevant, and when physical meaning for the reaction order is absent, interpretation of kinetic parameters is hazardous. Nonetheless by taking a series of compounds of known structure and comparing the parameters derived, it should be possible to make some meaningful comparisons and interpretations. In order to relate kinetic and thermodynamic data to a *mechanism* for the solid-state reaction or structural transformation, these processes should occur topotactically.[2,3] For only with knowledge of the crystallographic

†Georgetown University.
‡University of Zürich.

(1) (a) Sestâk, J.; Satava, V.; Wendlandt, W. W. *Thermochim. Acta* **1973**, *7*, 333–352. (b) Behnisch, J.; Schaff, E.; Zimmermann, H. *J. Therm. Anal.* **1978**, *13*, 117–128. (c) Coats, A. W.; Redfern, J. P. *Nature (London)* **1964**, *201*, 68–69. (d) Satava, V. *Thermochim. Acta* **1971**, *2*, 423–428.

(2) Following Günter and Oswald,[3a] we define a reaction as topotactic if the solid product is formed in one or only several definite crystallographic orientations relative to the parent crystal as a consequence of a chemical reaction or solid-state structural transformation and if it can proceed throughout the entire volume of the parent crystal. This definition differs in words only from several others.

0002-7863/84/1506-1669$01.50/0